

Supplementary Information

A novel ternary MQDs/NCDs/TiO₂ nanocomposite collaborated with activated persulfate for efficient RhB degradation under visible light irradiation

Qian Zhang ^a, Han Zhao ^a, Yuming Dong ^a, Xiangmiao Zhu ^a, Xiang Liu ^{a*}, Hexing Li ^{b*}

^a Key Laboratory of Synthetic and Biological Colloids, Ministry of Education, School of Chemical and Material Engineering, Jiangnan University, Wuxi 214122, P. R. China

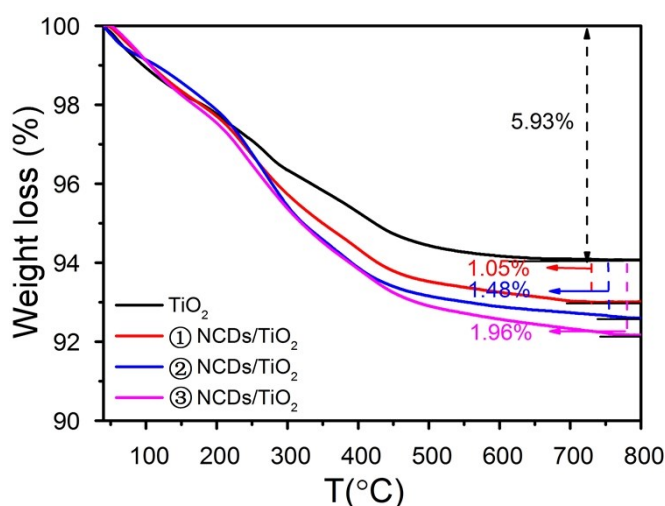
^b The Key Laboratory of the Chinese Ministry of Education in Resource Chemistry, Shanghai Normal University, Shanghai 200234, P. R. China

Content

Content 1. Thermogravimetric analysis of as-prepared NCDs/TiO ₂	S1
Content 2. Exploration of optimum loading amount of quantum dots on MQDs/NCDs/TiO ₂ nanocomposites	S2
Content 3. The morphology of NCDs and MQDs	S3
Content 4. The energy dispersive spectroscopy pattern and elements mapping of as-prepared sample	S4
Content 5. The specific surface area, average pore size and pore volume of three samples.....	S5
Content 6. Comparison of photocatalytic performance for MQDs/NCDs/TiO ₂ nanocomposites with similar materials	S6
Content 7. Band-gap energy and Valence-band XPS spectra of NCDs	S7

22 Content 1. Thermogravimetric analysis of as-prepared NCDs/TiO₂

23 Thermogravimetric analysis (TGA) was used to determine the amount of NCDs
24 loaded on TiO₂ nanosheets. As shown in the Fig.S1, the 5.93% weight loss in pure TiO₂
25 was mainly ascribed to the evaporation of adsorbed water, the decomposition of
26 surface-attached water, -OH group and remaining organic compound, while more
27 weight loss observed in NCDs/TiO₂ nanocomposites could result from the combustion
28 of NCDs. As a result, the mass percentage of NCDs in as-prepared three samples was
29 1.05%, 1.48% and 1.96%, respectively.



30

31 **Fig. S1** TGA curves of TiO₂ nanosheets and NCDs/TiO₂ with different NCDs content.

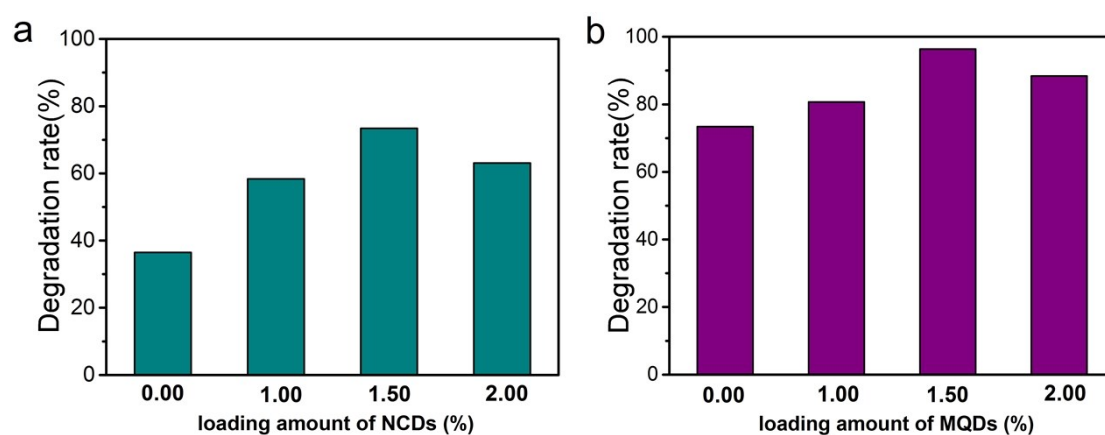
32

33

34 Content 2. Exploration of optimum loading amount of quantum dots 35 on MQDs/NCDs/TiO₂ nanocomposites

36 During the synthesis process of MQDs/NCDs/TiO₂ nanocomposites, NCDs were first

37 loaded on TiO₂ nanosheets. The photocatalytic activity of NCDs/TiO₂ with different
38 amounts of NCDs was evaluated toward RhB degradation to find the optimum content
39 of NCDs. The change tendency of degradation rate of RhB over NCDs/TiO₂
40 nanocomposites are shown in Fig. S2a and 1.5%NCDs/TiO₂ displays the highest
41 catalytic degradation activity. The decrease of photocatalytic activity with further
42 increasing of NCDs amount is probably because excessive NCDs will partially become
43 the recombination center of photogenerated electron-holes, which is disadvantageous to
44 photocatalytic degradation. On this basis, different amount of MQDs was further loaded
45 on 1.5%NCDs/TiO₂ nanocomposites. Similarly, the photocatalytic performance of
46 MQDS/NCDs/TiO₂ increases at first with the increase of MQDs content (Fig. S2b).
47 When the loading of MQDs was 1.5%, 1.5%MQDs/1.5%NCDs/TiO₂ exhibited the
48 highest photocatalytic activity. However, further increasing amount of MQDs brings
49 about a decrease of photocatalytic activity. This result may be ascribed to the shielding
50 effect of overcharged MQDs which will hinder the light absorption of NCDs/TiO₂.

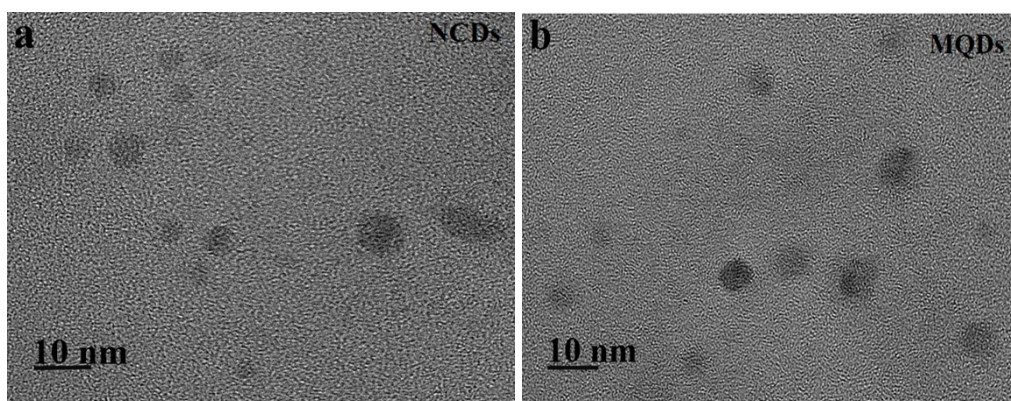


51

52 **Fig. S2** (a) The degradation rate of RhB by NCDs/TiO₂ nanocomposites loaded with different
53 amounts of NCDs, (b) the degradation rate of RhB by MQDs/NCDs/TiO₂ nanocomposites loaded
54 with 1.5% NCDs and different amounts of MQDs.

55 **Content 3. The HRTEM image of NCDs and MQDs**

56 The HRTEM image of NCDs and MQDs is shown in Fig. S3a and Fig. S3b,
57 respectively. It can be observed that NCDs and MQDs are both spherical and with the
58 dimensions less than 10 nm.



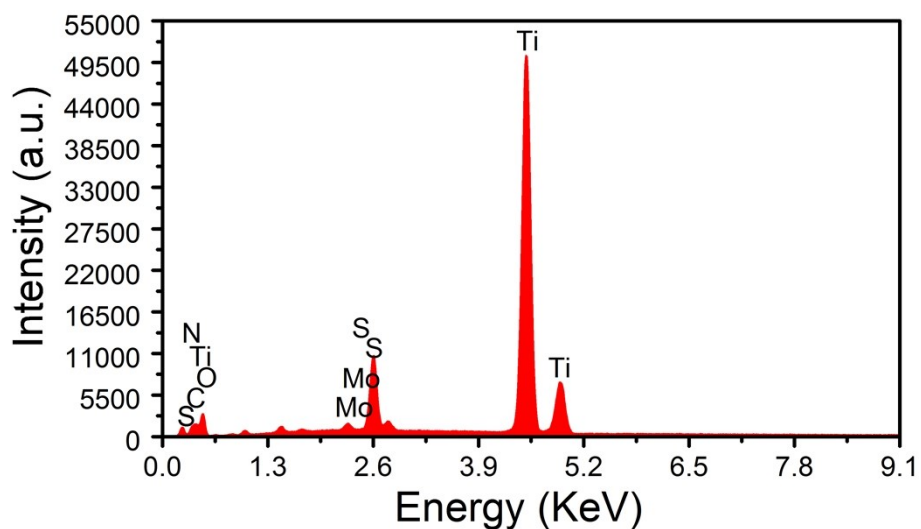
60 **Fig. S3** HRTEM image of (a) NCDs and (b) MQDs samples.

61

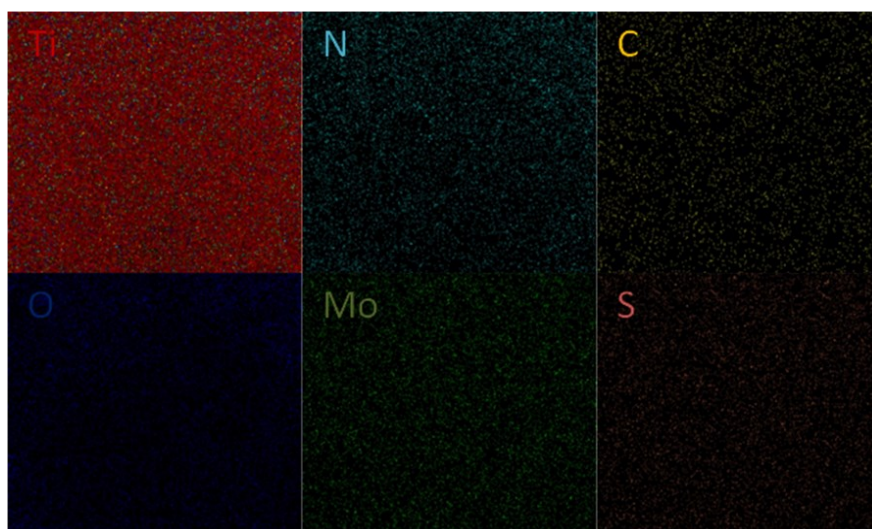
62

63 **Content 4. The energy dispersive spectroscopy pattern and elements**
64 **mapping of as-prepared sample**

65 The energy dispersive spectroscopy (EDS) pattern and elements mapping of sample
66 shows that the six elements of Ti, C, N, O, Mo and S were dispersed in
67 MQDs/NCDs/TiO₂ nanocomposites, which further demonstrates that NCDs and MQDs
68 were well distributed on TiO₂ nanosheets.



69



70

71 **Fig. S4** EDS pattern of MQDs/NCDs/TiO₂ nanocomposites and the corresponding elements mapping
 72 for Ti, N, C, O, Mo, and S.

73

74

75 **Content 5. The specific surface area, average pore size and pore**
 76 **volume of three samples**

77 The specific surface area, average pore size and pore volume of three samples were
 78 listed in Table S1.

79 **Table S1** Summary of specific surface area, average pore size and pore volume of TiO₂, NCDs/TiO₂
80 and MQDs/NCDs/TiO₂ samples.

Samples	Specific surface area (m ² /g)	Average pore size (nm)	Pore volume (cm ³ /g)
TiO ₂	126.13	17.87	0.049
NCDs/TiO ₂	116.71	17.01	0.045
MQDs/NCDs/TiO ₂	101.48	16.29	0.039

81

82

83 **Content 6. Comparison of photocatalytic performance for** 84 **MQDs/NCDs/TiO₂ nanocomposites with similar materials**

85 In this work, we compared nanocomposites with previously reported TiO₂-based
86 photocatalyst and the results listed in Table S2. The photocatalytic performance can be
87 influenced by some factors, such as the power of light source, the dose of catalysts and
88 pollutants, degradation time and so on. Compared with first three photocatalysts in
89 Table S2, the degradation efficiency of MQDs/NCDs/TiO₂ are the highest. Although the
90 degradation efficiency of MQDs/NCDs/TiO₂ is slightly lower than that of the latter two
91 catalysts, the degradation time and the power of light source are quite short and low.
92 Thus, the MQDs/NCDs/TiO₂ nanocomposites exhibit excellent photocatalytic activity
93 even without persulfate addition under visible light.

94 **Table S2** Comparison of photocatalytic performance for MQDs/NCDs/TiO₂ nanocomposites with
95 similar materials

Photocatalysts	Light source	Pollutant	Degradation time (min)	Degradation efficiency	Ref
CQDs/Fe ₂ O ₃ /TiO ₂ (50 mg)	Xe lamp (300 W)	MB (100 mL, 20 mg/L)	180	86.5 %	S1
CQDs/TiO ₂ / g-C ₃ N ₄ (50 mg)	Xe lamp (350 W)	Enrofloxacin (50 mL, 4 mg/L)	60	91.6 %	S2
MQDs/graphene/ TiO ₂ (40 mg)	Xe lamp (150 W)	RhB (80 mL, 10 mg/L)	80	80 %	S3
MoS ₂ /TiO ₂ /HMFs (400 mg)	Halogen lamp (500 W)	RhB (32 mL, 20 mg/L)	140	98.7 %	S4
C-Dots/Ag ₆ Si ₂ O ₇ /TiO ₂ (100 mg)	LED lamp (300 W)	RhB (250 mL, 8 mg/L)	120	99.8 %	S5
MQDs/NCDs/TiO ₂ (100 mg)	Xe lamp (150 W)	RhB (100 mL, 10 mg/L)	80	96.4 %	This work

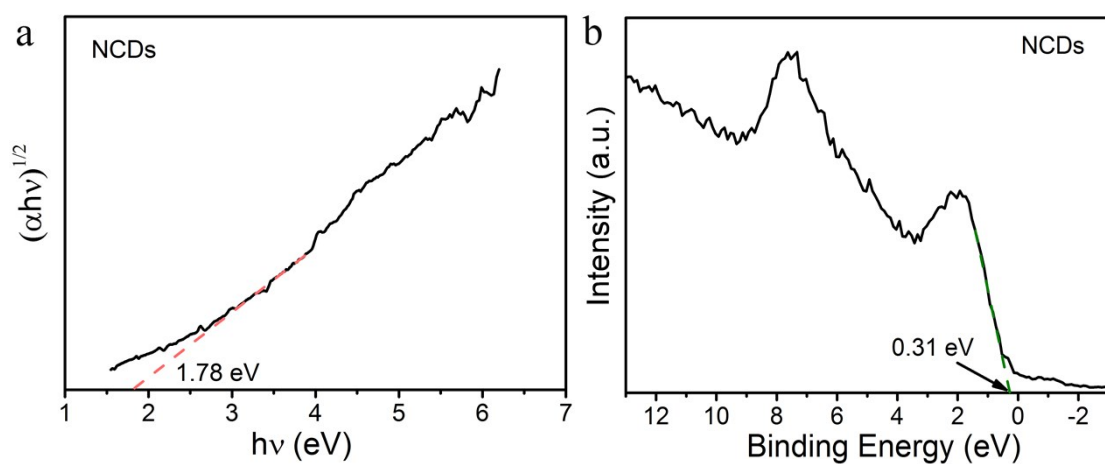
96 Reference:

- 97 S1. J. Zhang, M. Kuang, J. Wang, R. Liu, S. Xie, Z. Ji, Fabrication of carbon quantum
98 dots/TiO₂/Fe₂O₃ composites and enhancement of photocatalytic activity under visible light. *Chem.*
99 *Phys. Lett.*, 2019, **730**, 391-398.
- 100 S2. Y. Su, P. Chen, F. Wang, Q. Zhang, T. Chen, Y. Wang, K. Yao, W. Lv and G. Liu, Decoration
101 of TiO₂/g-C₃N₄ Z-scheme by carbon dots as a novel photocatalyst with improved visible-light
102 photocatalytic performance for the degradation of enrofloxacin. *RSC Adv.*, 2017, **7**, 34096-34103.
- 103 S3. W. Gao, M. Wang, C. Ran and L. Li, Facile one-pot synthesis of MoS₂ quantum dots-graphene-
104 TiO₂ composites for highly enhanced photocatalytic properties. *Chem. Commun.*, 2015, **51**, 1709-
105 1712.
- 106 S4. Y. Yu, J. Wan, Z. Yang and Z. Hu, Preparation of the MoS₂/TiO₂/HMFs ternary composite
107 hollow microfibres with enhanced photocatalytic performance under visible light. *J. Colloid Interf.*
108 *Sci.*, 2017, **502**, 100–111.
- 109 S5. S. Feizpoor, A. Habibi-Yangjeh, D. Seifzadeh, S. Ghosh, Combining carbon dots and Ag₆Si₂O₇
110 nanoparticles with TiO₂: Visible-light-driven photocatalysts with efficient performance for removal
111 of pollutants. *Sep. Purif. Technol.*, 2020, **248**, 116928-116938.

112

113 Content 7. Band-gap energy and Valence-band XPS spectra of NCDs

114 The band-gap and LUMO position of NCDs was determined from the plots of
115 $(\alpha h\nu)^{1/2}$ versus band-gap energy and valence-band XPS spectrum. As shown in Fig. S5a
116 and Fig. S5b, the band-gap of NCDs is about 1.78 eV and the HOMO position is at 0.31
117 eV. Based on this, the LUMO position can be calculated to be -1.47 eV.



118
119 Fig. S5 (a) Band-gap energy and (b) valence-band XPS spectrum of NCDs

120